Methodology for the elaboration of the design table of GFRP structures subjected to fire

Harkaitz García[1]*, Mikel Zubizarreta[2] and Iñaki Garmendia[1]

[1]Mechanical Engineering Department, Faculty of Engineering Gipuzkoa, University of the Basque Country UPV/EHU, Plaza de Europa, 1 20018) Donostia-San Sebastián, Spain
**arkaitz.garcia@ehu.eus*

[2]Bussines Organization Department, Faculty of Engineering Gipuzkoa, University of the Basque Country UPV/EHU, Plaza de Europa, 1 20018) Donostia-San Sebastián, Spain

"This is an accepted manuscript of an article published by Taylor & Francis in Mechanics of Advanced Materials and Structures on 16 October 2021, available at: https://doi.org/10.1080/15376494.2021.1980924."

ARTICLE TEMPLATE

Methodology for the elaboration of the design table of GFRP structures subjected to fire

H. García[a], M. Zubizarreta[b] and I. Garmendia[a]

[a]Mechanical Engineering Department, Faculty of Engineering Gipuzkoa, University of the Basque Country UPV/EHU, Plaza de Europa, 1 20018) Donostia-San Sebastián, Spain; [b]Bussines Organization Department, Faculty of Engineering Gipuzkoa, University of the Basque Country UPV/EHU, Plaza de Europa, 1 20018) Donostia-San Sebastián, Spain

ARTICLE HISTORY
Compiled September 1, 2021

ABSTRACT
The main objective of this study is to establish a fire protection design method for pultruded Glass Fiber Reinforced Polymer (GFRP) structures exposed to fire. The method is based on the development of tables similar to those already available for steel structures. The structural designer may use these tables to determine the minimum required thickness (of any type of insulation), so that the structure maintains its mechanical properties above the over-dimensioning coefficient. The method used to draw up these tables follows four steps; i) First, the limit temperatures are determined or the temperature ranges within which the application of pultruded GFRP is permitted; ii) Second, the behavior of certain physical properties (density, specific heat, thermal conductivity, emissivity...) are defined as a function of the temperature; iii) Third, the method to determine the fire resistance temperature of the pultruded profile sections is defined; iv) Finally, the mechanical properties and ultimate resistance values of these profiles at different temperatures are also estimated. The behavior of the mechanical properties is analyzed as a function of the massivity of each section and the ratio between the thermal conductivity of the insulation and its thickness. In addition, a practical example is given of the application of the tables to a pultruded GFRP structure.

KEYWORDS
Pultruded elements; Fire protection; dimensioning method

1. Introduction

One main limitation of pultruded Glass Fiber Reinforced Polymer (GFRP) profiles in building and bridge structures is their poor performance when exposed to fire Wong, Davies, and Wang (2004); Rosa et al. (2018, 2019). The authors of this paper nevertheless believe that there should be some rules or standards for its design, as is indeed the case of other structural materials.

Among the characteristics of pultruded GFRP profiles is that most of them should be classified as class 4 sections, as in Eurocode 3, if analyzed in a similar way to steel CEN (2005).

At room temperature, Class 4 sections have different and more complex characteristics than Class 1, 2 and 3 sections, mainly due to the likelihood of local buckling within

CONTACT H. García. Email: arkaitz.garcia@ehu.eus

the section. A behavior that necessitates specific design rules and their corresponding design methods, which are already well established in the case of steel CEN (2005). Design methods are likewise under development for pultruded components Ascione et al. (2016).

At higher temperatures (fire situations), Class 4 steel sections are usually oversized in most buildings Couto et al. (2016); Knobloch et al. (2012); Couto et al. (2018); Maia et al. (2016), due to the fact that, in practice, they are limited to the critical temperature of 350ºC CEN (2005), when, in reality, they could continue to work at higher temperatures Franssen, Zhao, and Gernay (2016); Jandera, Prachař, and Wald (2020); Prachar et al. (2015).

Up until now, different countries have had their own design guidelines for Fiber Reinforced Polymer (FRP) structures, i.e., Germany BUE (2010), Italy Council et al. (2007), the Netherlands CUR Commission C124 (2003) and the United States Association et al. (2012). No specific procedures have been proposed for design at elevated temperatures in these guidelines, while design rules are available for steel Eurocode (1993), concrete del Hormigón Estructural (2008) and wood for Standardization (CEN). Moreover, there are no specific fire protection design procedures in the draft versions of the future Eurocode for FRP Ascione et al. (2016). This future standard needs to make a contribution in this respect Maraveas, Miamis, and Vrakas (2012)

In this study, a design method is proposed for pultruded GFRP components. A table is presented to obtain the minimum insulation thickness necessary to achieve the mechanical properties required for each section of the structure.

The tables were calculated for fire resistance times of less than 60 minutes. While investigating these values, it was concluded that longer exposure times were not viable for coatings of reasonable thickness. The tables were therefore not limited to the standard intervals of 30, 60, and 90 minutes. Instead, they were organized into shorter periods, from 5 to 60 minutes, in 5-minute increments.

The discretization of time periods can be useful for optimization of the fire design of structures, although it requires specific calculations and the adjustment of the "requested standard times". The equivalent time equation is one suggested method that could be used Eurocode (2002).

2. Methodology

The steps taken to obtain the tables presented in the design method proposed in this article are explained below (Figure 1):

The symbols used in this article are presented below:

- Tg:glass transition
- Td:decomposition temperature
- Em: modulus of elasticity
- Eg: glassy modulus
- Er: rubbery modulus
- αg :conversion degree of the glass transition
- ρ :density
- cp: specific heat
- ϵ: emissivity
- λ: thermal conductivity
- d: coating thickness

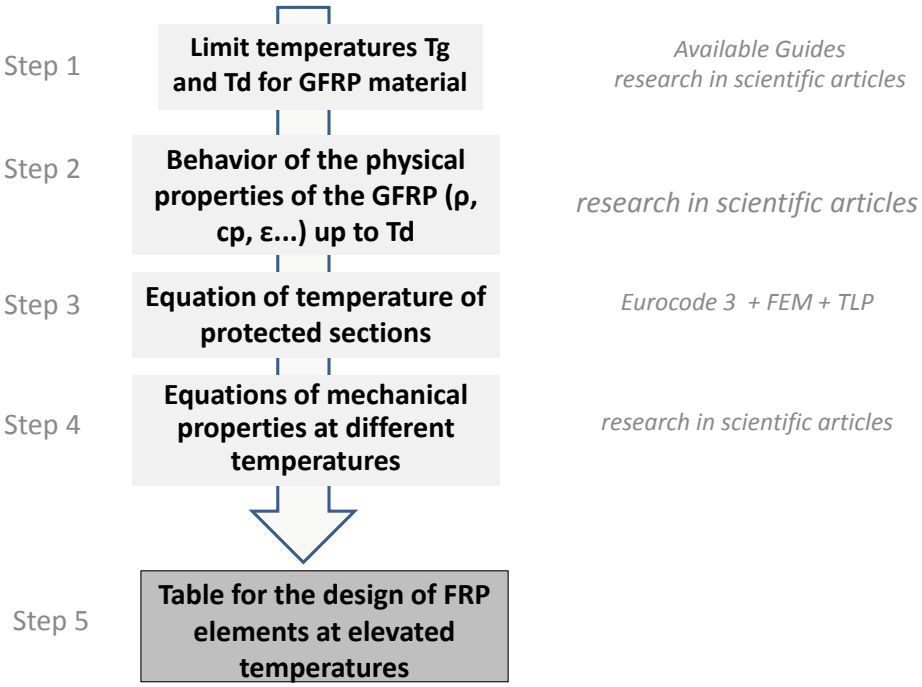

Figure 1. Methodology for the development of the table

- λp: effective thermal conductivity of the coating

2.1. *Step 1: Limit temperatures for pultruded GFRP material.*

In this first step, our aim was to determine the temperature range in which the pultruded GFRP material may be used in structures. To do so, a bibliographical search of articles and existing guides was performed.

Bai et al. Bai and Keller (2007) stated that the elastic Young's modulus underwent a considerable (although recoverable) decrease during its glass transition at Tg temperature. They also stated that, although the moduli of longitudinal and transverse elasticity were different in this type of material, the decrease was similar for values between the glass transition temperature, Tg and the decomposition temperature, Td Bai et al. (2008). These reasons explain why the existing guidelines limit the use of GFRP to temperatures close to Tg. Taking the data of common pultruded GFRP material used in the work of Morgado et al. Morgado et al. (2018); Morgado, Silvestre, and Correia (2018a,b) (Tg=141$^{\text{o}}$C, Td=370$^{\text{o}}$C) as a reference, the limit temperatures of some guides might be as follows:

- ASCE Association et al. (2012): Tg-22 = 141 – 22= 119 $^{\text{o}}$C
- German guideline BUE (2010): Tg-15 = 141 – 15= 126 $^{\text{o}}$C
- Dutch CUR Commission C124 (2003): Tg-20 = 141 – 20= 121 $^{\text{o}}$C

Using a mean Tg $\simeq 120^{\text{o}}$C

In the specific design procedure for pultruded GFRP structures discussed in this article, three design ranges are proposed depending on the temperature of the section:

- Zone 1 (white): $\theta < 120^{\text{o}}$C
- Zone 2 (light grey): $120^{\text{o}}\text{C} \leq \theta \leq 370^{\text{o}}$C
- Zone 3 (dark grey): $\theta > 370^{\text{o}}$C

In Zone 1 it is possible to calculate the structures without modifying their elastic moduli. In Zone 2 the elastic moduli should be corrected using those values corresponding to the real temperature of the section. the equation presented by Bai et al. Bai, Keller, and Vallée (2008) (1) is proposed to obtain the modulus of elasticity. Finally, it is not advisable to design pultruded GFRP structures within the range corresponding to Zone 3.

$$E_m = E_g \cdot (1 - \alpha_g) + E_r \cdot \alpha_g \cdot (1 - \alpha_g) \tag{1}$$

where, Em is the modulus of elasticity, Eg and Er are the glassy and rubbery modulus, respectively, and αg$\cdot$ is the conversion degree of the glass transition.

Figure 2 shows the three zones for different section sizes.

2.2. *Step 2: Behavior of the physical properties of pultruded GFRP material.*

In Step 2, a bibliographic search was conducted for data that reflect the behavior of the material properties as a function of the temperature: density ρ, specific heat cp, emissivity ϵ and thermal conductivity λ, of the pultruded GFRP materials up to the limit temperatures obtained in Step 1.

50 m⁻¹	time (min)											
d/λp	5	10	15	20	25	30	35	40	45	50	55	60
0.05	338	512	613	673	708	732	757	802	855	891	917	936
0.1	185	347	453	529	586	630	663	688	706	720	734	748
0.15	98	237	342	420	480	530	571	605	633	657	676	691
0.2	50	154	252	330	393	444	487	525	557	585	610	631
0.25	34	92	177	252	315	368	413	452	486	516	543	567
0.3	34	53	116	185	246	299	345	385	421	452	480	506
0.35	34	35	71	127	183	235	281	322	359	391	421	447
0.4	34	34	43	81	129	177	221	262	299	333	363	391
0.45	34	34	34	50	84	125	167	206	243	277	308	336
0.5	34	34	34	36	53	83	118	155	190	223	254	283
0.55	34	34	34	34	37	53	79	109	141	172	203	231
0.6	34	34	34	34	34	37	51	73	99	127	155	182

200 m⁻¹	time (min)											
d/λp	5	10	15	20	25	30	35	40	45	50	55	60
0.05	557	709	783	880	923	946	960	970	977	983	987	992
0.1	319	541	653	710	748	800	854	891	917	936	951	962
0.15	124	362	504	596	658	699	727	753	786	825	856	880
0.2	34	188	347	457	537	598	645	680	706	727	746	767
0.25	34	56	187	309	402	475	533	581	620	653	680	701
0.3	34	34	60	158	257	341	409	465	513	554	589	619
0.35	34	34	34	48	116	198	273	337	393	441	482	519
0.4	34	34	34	34	36	73	134	199	260	315	363	406
0.45	34	34	34	34	34	34	41	76	126	180	231	279
0.5	34	34	34	34	34	34	34	34	39	65	103	146
0.55	34	34	34	34	34	34	34	34	34	34	35	48
0.6	34	34	34	34	34	34	34	34	34	34	34	34

100 m⁻¹	time (min)											
d/λp	5	10	15	20	25	30	35	40	45	50	55	60
0.05	450	629	705	746	812	879	917	941	957	969	977	984
0.1	254	450	564	638	685	714	737	761	802	846	878	903
0.15	121	310	433	519	583	632	668	694	713	729	745	764
0.2	47	190	316	409	480	536	582	619	649	674	693	708
0.25	34	95	208	304	381	442	492	535	571	603	629	652
0.3	34	41	116	205	284	349	404	450	490	525	556	583
0.35	34	34	53	118	191	257	315	365	409	447	480	511
0.4	34	34	34	56	110	170	227	279	325	366	403	436
0.45	34	34	34	34	53	95	145	195	242	285	324	359
0.5	34	34	34	34	34	46	78	118	161	203	243	280
0.55	34	34	34	34	34	34	39	60	92	128	165	201
0.6	34	34	34	34	34	34	34	35	46	68	96	128

250 m⁻¹	time (min)											
d/λp	5	10	15	20	25	30	35	40	45	50	55	60
0.05	588	728	832	904	935	953	964	972	978	984	988	992
0.1	335	564	674	727	774	838	882	911	932	948	960	970
0.15	114	370	519	613	675	714	743	777	818	851	877	898
0.2	34	171	343	461	545	608	656	692	718	740	763	790
0.25	34	39	158	290	392	471	533	584	625	660	687	709
0.3	34	34	37	116	222	313	389	451	503	547	585	618
0.35	34	34	34	34	68	145	225	298	360	414	460	501
0.4	34	34	34	34	34	37	73	134	199	259	314	363
0.45	34	34	34	34	34	34	34	35	58	102	153	205
0.5	34	34	34	34	34	34	34	34	34	34	39	63
0.55	34	34	34	34	34	34	34	34	34	34	34	34
0.6	34	34	34	34	34	34	34	34	34	34	34	34

150 m⁻¹	time (min)											
d/λp	5	10	15	20	25	30	35	40	45	50	55	60
0.05	514	682	742	829	895	930	950	963	973	980	985	990
0.1	294	506	620	686	722	753	799	850	886	912	931	946
0.15	128	345	478	568	632	676	706	728	749	776	812	844
0.2	39	196	341	443	518	577	623	659	687	708	725	741
0.25	34	78	206	316	401	468	523	568	606	637	664	685
0.3	34	34	91	190	280	355	416	468	512	549	582	611
0.35	34	34	35	84	162	238	305	362	411	454	492	525
0.4	34	34	34	35	67	126	191	251	305	352	395	432
0.45	34	34	34	34	34	49	90	142	195	245	291	332
0.5	34	34	34	34	34	34	36	58	95	139	183	226
0.55	34	34	34	34	34	34	34	34	38	58	88	124
0.6	34	34	34	34	34	34	34	34	34	34	36	50

300 m⁻¹	time (min)											
d/λp	5	10	15	20	25	30	35	40	45	50	55	60
0.05	611	743	860	916	941	956	966	973	979	985	989	993
0.1	345	581	689	741	802	860	897	922	941	954	965	973
0.15	100	371	526	623	686	724	757	798	836	866	889	908
0.2	34	148	331	457	546	612	662	699	725	749	776	805
0.25	34	34	123	263	374	459	526	580	624	660	690	713
0.3	34	34	34	74	176	276	359	428	485	533	574	609
0.35	34	34	34	34	37	88	167	246	315	376	428	473
0.4	34	34	34	34	34	34	36	69	126	190	250	306
0.45	34	34	34	34	34	34	34	34	34	41	73	119
0.5	34	34	34	34	34	34	34	34	34	34	34	34
0.55	34	34	34	34	34	34	34	34	34	34	34	34
0.6	34	34	34	34	34	34	34	34	34	34	34	34

Figure 2. Design tables, zones 1, 2 and 3 for different section sizes

According to Correia et al. Correia, Bai, and Keller (2015), the thermo-physical properties (density, specific heat and thermal conductivity) remain stable until the decomposition temperature of the material (Td). However, Bai et al. proposed equations as a function of temperature that define the behavior of the thermal conductivity λ Bai et al. (2008), the specific heat ratio and the density Yu, Till, and Thomas (2007). Although Keller et al. also analyzed and proposed a linear progression for the emissivity coefficient Keller, Tracy, and Zhou (2006), it was decided to use the equations of Bai et al. to obtain the tables presented in this article.

2.3. *Step 3: Temperature calculation for pultruded GFRP beams exposed to fire.*

Eurocode 3, parts 1-2 is only applicable to steel structures exposed to fire Eurocode (1993). The formulae that appear in that context are therefore limited to these metal components. However, it appears highly desirable to have a set of equivalent formulae that could be used for pultruded GFRP beams and columns. The method followed to develop such a set of formulae was to investigate the basic assumptions of the EC-3 norm, in order to establish whether they are applicable to the case of pultruded GFRP.

2.3.1. Assumptions for steel sections

The main assumption of the EC-3 norm is that, if the exposure and the insulation are equal on all exposed surfaces, then the temperature of an insulated steel structure exposed to fire may be estimated by a one-dimensional analysis. At the same time, the corner effects are neglected. In addition, as the thermal diffusivity of steel is very high, it can be assumed that the heat will be uniformly distributed throughout the steel Wickström (1985).

An HEB-300 steel section was used as a case study to verify these assumptions. The steel section was insulated with a 25 mm rock wool layer. Three different numerical methods were used to calculate the temperatures distribution over time: the TLP (Thermal Lumped Parameter) method Associates (2019); Garmendia et al. (2016), the formula (4.27) from EC-3 Eurocode (1993) and the well-established Finite Element Method. The temperature of the fire was taken from the ISO 834 curve Standard (1999), as shown in (2):

$$\theta_g = 20 + 345 \cdot log\,(8t + 1) \tag{2}$$

where, t is expressed in minutes and θg in ^{o}C.

The first method, the TLP method, assumes a two-node network model (gas node number 1 and steel node number 2) with a single linear conductance between both (GL(1,2)=0.71120 W/^{o}C). This linear conductance is the inverse value of the thermal resistance that is present due to the insulation layer. The steel is assumed to have a single temperature (at node 2) with a thermal inertia of M2C2=16817.055 J/^{o}C. The temperature at node 1 is imposed as a boundary condition and as a function of time. The program (called TK) calculates temperature at node 2 as a function of time, producing a numerical solution to the differential equation (3):

$$GL\,(1,2)\,(T_1 - T_2) + M_2 C_2 \frac{dT_2}{dt} = 0 \tag{3}$$

The second method integrates the equation in EuroCode-3 CEN (2005) over time (4):

$$\Delta\theta_{a,t} = \frac{\lambda_p A_p / V\,(\theta_{g,t} - \theta_{a,t})}{d_p c_a \rho_a\,(1 + \phi/3)} \Delta t - \left(e^{\phi/10} - 1\right) \Delta\theta_{g,t} \tag{4}$$

following the method suggested in Franssen, Kodur, and Zaharia (2009).

Finally, the Finite Element Method was used to model a quarter of the HEB section, which is sufficient due to geometry and loads symmetries. The mesh shown in Figure 3 was used where the different materials (steel and insulation) are color coded.

The results of the three methods are summarized below in Figure 4.

The results of the three methods compare well. For the FEM method, a temperature distribution on the section (differences lower than 12 ^{o}C, see Figure 5) was calculated with the FEM method and a mean temperature value was used for the comparisons.

From these results, it is possible to state that the three methods could be used to estimate the steel temperature and that the assumption of a single temperature representing the thermal state of the steel is appropriate.

2.3.2. Assumptions for pultruded GFRP material

The idea is now to use the three previously mentioned methods to estimate the GFRP temperature as a function of time, so as to evaluate whether the assumption of a single temperature that represents the thermal state of the GFRP is appropriate.

Pultruded GFRP material properties were used as a function of the temperature, obtained from the prospect for new guidance Ascione et al. (2016). The results are summarized in Figure 6.

Reasonable comparisons between the three curves were evident with temperature values that were higher than those assumed for the steel section. The pultruded GFRP section presented quite large gradients, as can be seen in Figure 7.

The mean value of the FEM results reflected in Figure 6 provided a reasonable representation of the thermal state of the whole pultruded GFRP section. However, if the maximum temperature in the section is analyzed, it is far off the mean value (those calculated with any of the three methods); a difference that was larger as the exposure time increased.

2.3.3. Relation between TEC-3 and Tmax FEM

The thermal conductivity of pultruded GFRP is much lower than steel. This fact results in differences between the maximum and the mean temperatures of the GFRP sections. This difference is more evident for sections with the fewest faces exposed to fire where the low conductivity of GFRP plays an important role. The fewer the number of faces exposed to fire, the larger the difference between the maximum temperature within the section and that obtained with eq. (4).

The number of different cases that can be devised with different section geometries and the number of faces exposed to fire is extremely high. As a consequence, it was

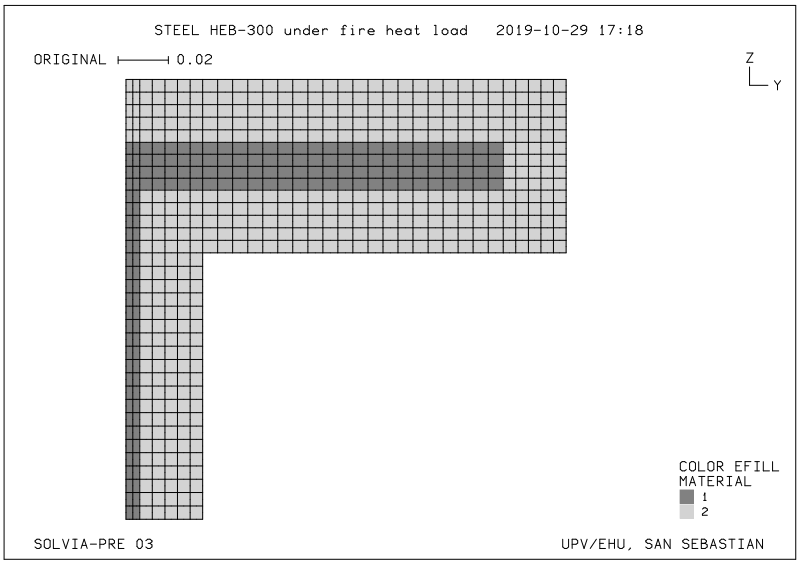

Figure 3. Mesh and materials of a HEB-300 case study

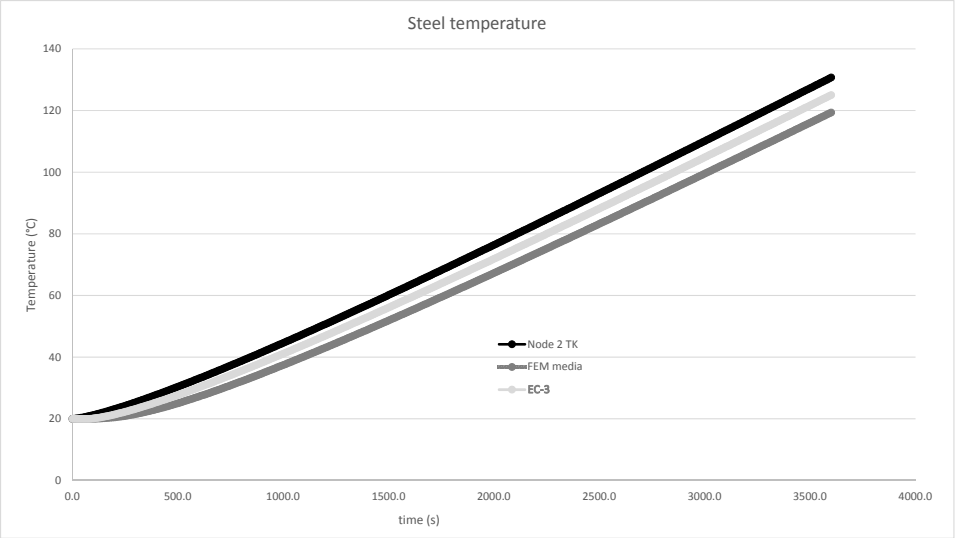

Figure 4. Comparison of steel temperatures as a function of time with three methods

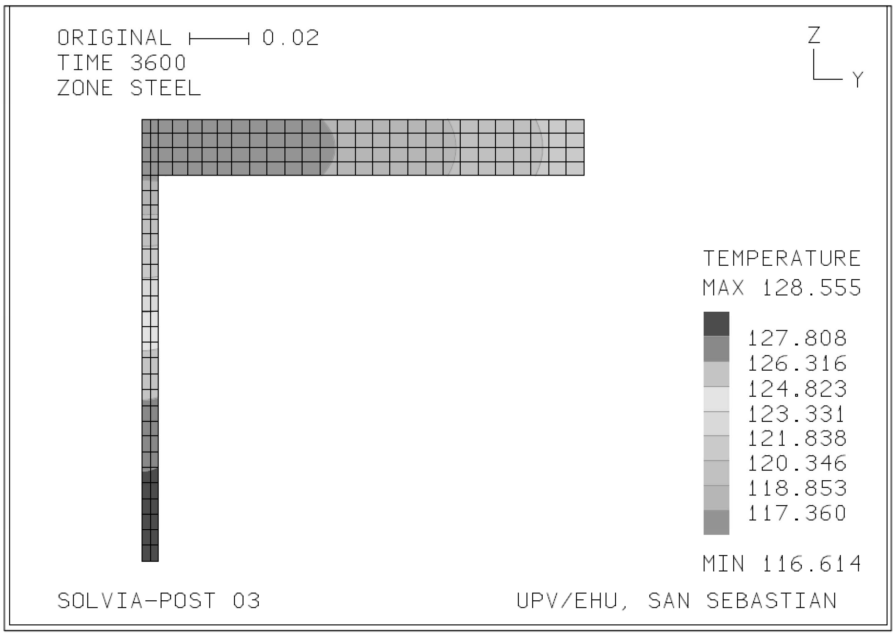

Figure 5. Temperature distribution after 1 hour for the steel and insulation

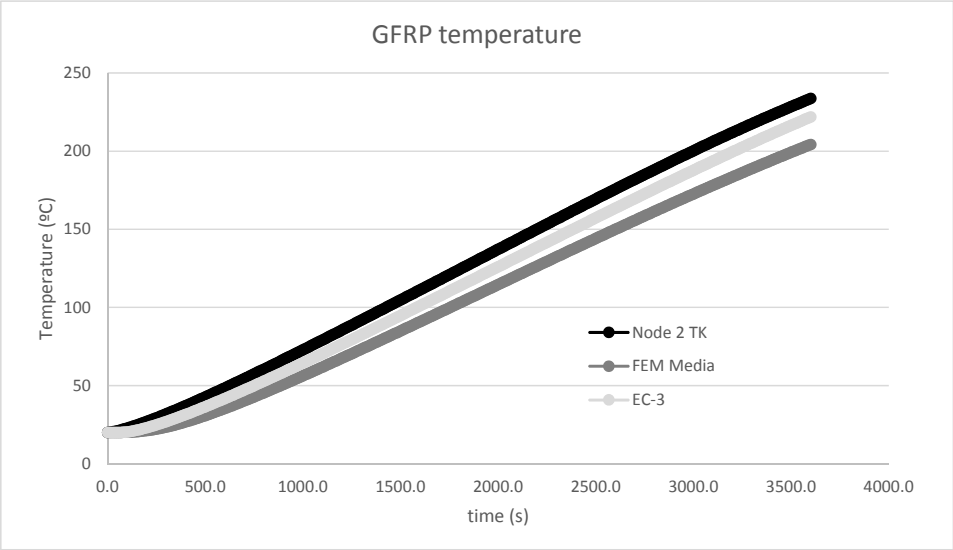

Figure 6. Comparison of GFRP temperatures as a function of time with three methods

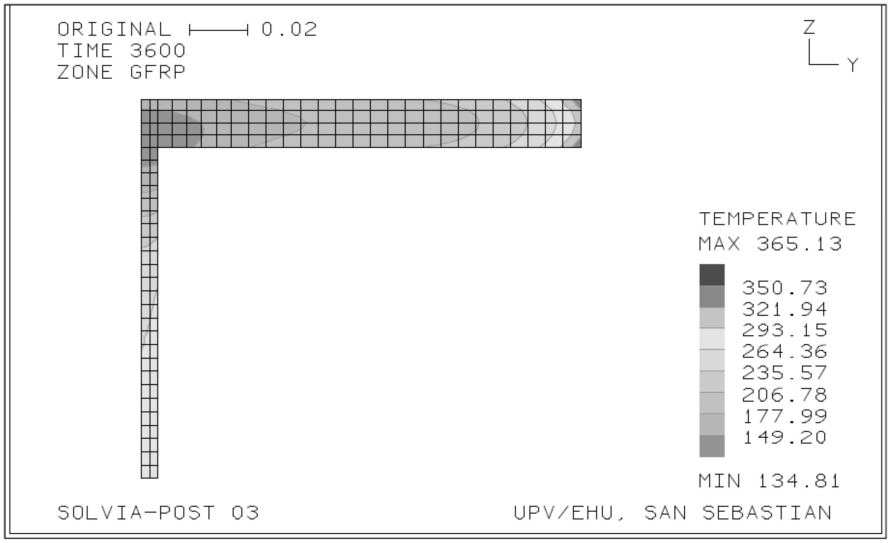

Figure 7. Temperature distribution after 1 hour for the GFRP and insulation

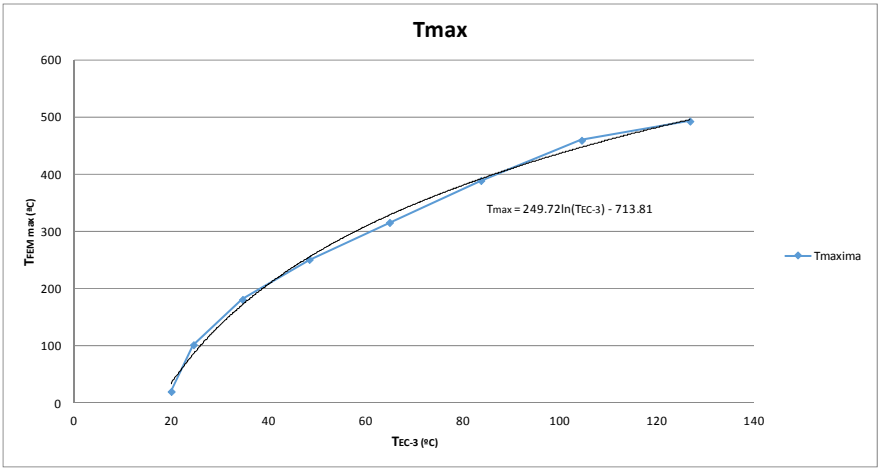

Figure 8. Tmax EC-3 correction curve

decided to focus only on the structures exposed on all four faces. The preparation of the corresponding tables for components exposed to one, two or three faces will be the subject of a future study.

A description of the procedure followed to take into account the temperature difference between TEC-3 (calculated with eq. (4)) and Tmax FEM will now be given. In short, one correction will be applied to each TEC-3 temperature (within the application range of the pultruded GFRP material from 20ºC to 370ºC).

It was decided to analyze the most unfavorable scenario: i.e., where the most important temperature differences will occur within the section, in order to assess the correction that has to be applied, as the casuistry of possible section types (pipes, squares, IPE, HEB, etc.) is very extensive. The search for these section types led us to consider double-T open sections with large flange thicknesses (HEM), moderate massivity (large HEM320 sections) and quick heating (without insulation).

Figure 8 shows the logarithmic equation (5) that is best adapted to the results. TEC-3 was calculated with eq. (4) and then Tmax with eq. (5). The value of Tmax was used as a reference temperature for the preparation of the design tables presented in this article.

$$T_{max} = 249.72 \times ln\left(T_{EC-3}\right) - 713.81 \tag{5}$$

2.4. *Step 4: Mechanical properties at different temperatures.*

A bibliographic search was conducted to obtain the equations proposed to date that determine tensile, shear, longitudinal compression and transverse compression strengths as a function of section temperature for the pultruded GFRP material.

The equations finally used due to their lower "absolute mean percentage errors" (AMPE) were those of Wang et al. Wang, Young, and Smith (2011) (6) for tensile and compression, and that of Correia et al. Correia et al. (2013) (7) for shear.

$$P\left(T\right) = P_u \times \left[A - \frac{\left(T - B\right)^n}{C}\right] \tag{6}$$

$$P\left(T\right) = \left(1 - e^{Be^{C \times T}}\right) \times \left(P_u - P_r\right) + P_r \tag{7}$$

in which P is the mechanical property with temperature T, Pu is the property at ambient temperature, Pr is the mechanical property after glass transition and coefficients A, B, C and n can be estimated for different temperature ranges.

2.5. *Step 5: Design table calculation.*

Eq. (4) was combined with eqs. (6) and (7) in each case for the design tables proposed for pultruded GFRP profiles with different section sizes, different fire exposure times and different conductivity and protection thickness ratios. The maximum temperature was obtained using the corrector eq. (5) that considers the temperature gradient within the section.

3. Results

Table 1 is the result of the implementation of the methodology presented in the previous section.

This table shows the value of the protection coefficient, d/λ, to be applied to the section, so that the reduction in tensile (t), shear(s) and compressive(c) strength will be lower than the limit obtained after the structural calculation (in extraordinary fire situations).

The input data for this table are the required fire exposure time in minutes (R5, R10, R15, ...), the form factor (Am/V) and the minimum required resistances. The output data are the value of the protection coefficient d/λ, i.e., the ratio between thermal conductivity and the required insulation thickness.

In addition, this table will indicate the Zone (1 or 2) in which the section is found (in reference to step 1 of the previous section). If it turns out that the structure has to work in Zone 2, it will be necessary to make a readjustment of the modulus of elasticity following the corresponding equation (1).

Table 1. Compressive, shear ant tensile strenght. Protection coefficient d/λ (m2K/W).

Protection coefficient d/λ (m²K/W)										
Standard-time fire resistance	Form factor A_m/V	Oversizing Coefficient > $\mu_{fi,c}$			Oversizing Coefficient > $\mu_{fi,s}$			Oversizing Coefficient > $\mu_{fi,t}$		
		$0.7 \geq \mu_{fi,c} > 0.55$	$0.55 \geq \mu_{fi,c} > 0.4$	$0.4 \geq \mu_{fi,c} > 0.25$	$0.7 \geq \mu_{fi,s} > 0.55$	$0.55 \geq \mu_{fi,s} > 0.4$	$0.4 \geq \mu_{fi,s} > 0.25$	$0.7 \geq \mu_{fi,t} > 0.6$	$0.6 \geq \mu_{fi,t} > 0.5$	$0.5 \geq \mu_{fi,t} > 0.4$
R5	30	0.2	0.15	0.15	0.2	0.15	0.15	0.1	0.1	0.05
	50		0.2			0.2				0.1
	100			0.2			0.2	0.15	0.15	
	150									0.15
	200			0.15						
	250						0.15			
	300									
R10	30	0.3	0.25	0.25	0.3	0.25	0.25	0.15	0.15	0.1
	50		0.3			0.3		0.2	0.2	0.15
	100							0.25		
	150		0.25			0.25				0.2
	200	0.25			0.25			0.2		
	250									
	300									
R15	30	0.35	0.35	0.3	0.4	0.35	0.3	0.25	0.2	0.15
	50				0.35		0.35		0.25	0.2
	100		0.3					0.3		
	150									0.25
	200	0.3			0.3	0.3	0.3	0.25		
	250									
	300									
R20	30	0.45	0.4	0.35	0.45	0.4	0.4	0.3	0.25	0.2
	50			0.4				0.35	0.3	0.25
	100	0.4			0.4					
	150		0.35	0.35		0.35	0.35	0.3		0.3
	200	0.35			0.35					
	250			0.3						
	300	0.3	0.3			0.3	0.3			0.25
R25	30	0.5	0.45	0.4	0.5	0.45	0.45	0.35	0.3	0.25
	50			0.45					0.35	0.3
	100	0.45		0.4	0.45		0.4			0.35
	150	0.4	0.4			0.4				
	200			0.35	0.4					0.3
	250	0.35	0.35			0.35	0.35		0.3	
	300				0.35			0.3		
R30	30	0.55	0.5	0.45	0.55	0.55	0.5	0.4	0.35	0.3
	50			0.5		0.5			0.4	0.35
	100	0.5		0.45	0.5		0.45			
	150	0.45	0.45		0.45	0.45				
	200	0.4	0.4	0.4			0.4		0.35	
	250				0.4	0.4		0.35		
	300		0.35	0.35			0.35			0.3
R35	30	0.6	0.55	0.5	0.6	0.6	0.55	0.4	0.4	0.35
	50					0.55		0.45		
	100	0.55	0.5		0.55	0.5	0.5			0.4
	150	0.5	0.45	0.45	0.5		0.45			
	200	0.45			0.45	0.45		0.4		
	250	0.4	0.4	0.4			0.4		0.35	0.35
	300				0.4	0.4		0.35		
R40	30	-	0.6	0.55	-	0.6	0.55	0.45	0.4	0.35
	50	0.6						0.5	0.45	0.4
	100	0.55	0.55	0.5	0.55	0.55				0.45
	150	0.5	0.5		0.5	0.5	0.5	0.45		
	200		0.45	0.45		0.45	0.45		0.4	0.4
	250	0.45			0.45			0.4		
	300	0.4	0.4	0.4		0.4	0.4			0.35
R45	30	-	-	0.6	-	-	0.6	0.5	0.45	0.4
	50								0.5	0.45
	100	0.6	0.55	0.55	0.6	0.6	0.55			
	150	0.55		0.5	0.55	0.55	0.5		0.45	
	200	0.5	0.5		0.5	0.5		0.45	0.45	
	250	0.45	0.45	0.45	0.45	0.45	0.45		0.4	0.4
	300							0.4		
R50	30	-	-	-	-	-	-	0.55	0.5	0.45
	50									0.5
	100	0.6	0.6	0.6		0.6	0.6			
	150	0.55	0.55	0.55	0.55	0.55	0.55	0.5		0.45
	200	0.5	0.5	0.5	0.5	0.5	0.5	0.45	0.45	
	250			0.45			0.45			0.4
	300	0.45	0.45		0.45	0.45		0.4	0.4	
R55	30	-	-	-	-	-	-	0.55	0.5	0.45
	50							0.6	0.55	
	100			0.6				0.55		0.5
	150	0.6	0.55	0.55	0.6	0.6	0.55			
	200	0.55		0.5	0.55	0.55	0.5	0.5	0.5	
	250	0.5	0.5		0.5	0.5				0.45
	300	0.45	0.45	0.45		0.45	0.45	0.45	0.45	
R60	30	-	-	-	-	-	-	0.6	0.55	0.5
	50									0.55
	100									
	150	0.6	0.6	0.6	0.6	0.6	0.6	0.55	0.5	0.5
	200	0.55	0.55	0.55	0.55	0.55	0.55	0.5		
	250	0.5	0.5	0.5	0.5	0.5	0.5		0.45	0.45
	300			0.45				0.45		

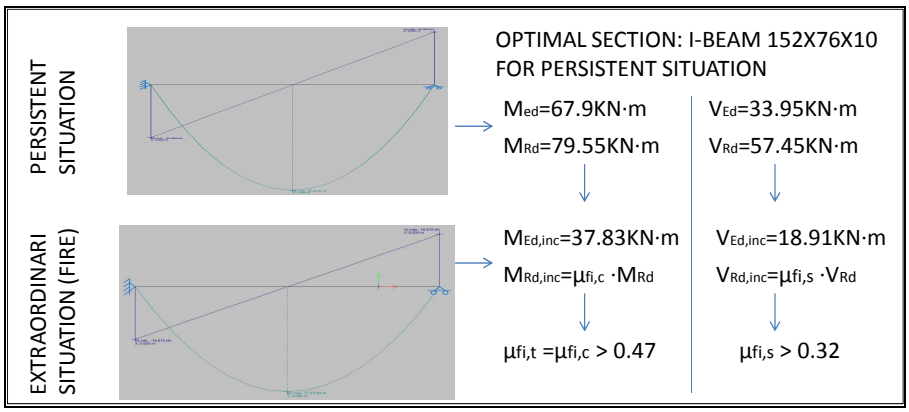

Figure 9. Design and resistant moments and shears for persistent and extraordinary situations (fire)

4. Results analysis

4.1. *Application example*

An illustration of how this design methodology should be applied is described below. The thickness of "gypsum plasterboard" insulation (λ =0.2 W/m^{o}C) will be calculated for the joist of a floor slab, with simple end supports, a span of 8 meters, a distance between the beams of 0.85 m, slab weight + pavement 4KN/ m2, usage overload 3KN/ m2 and a fire resistance of 30 minutes.

In Figure 9, the calculation and the optimization of the beam is summarized for persistent situations and it presents the real stresses with the minimum oversized coefficients for an extraordinary fire situation.

Using the design table presented in this study, Figure 10 shows the ratio between the thermal conductivity of the section and the required minimum insulation thickness of 0.4 m2K/W. The ratio was obtained both for the compression strength (derived from the bending moment) and for the tangential strength (derived from the shear). It therefore requires a minimum insulation thickness of 0.08m of the "plasterboard" type.

However, a value of 0.35 m2K/W is sufficient for the tensile stress (derived from the bending moment), which means that the traction wing could be protected with a lower thickness of 0.07m. However, it will be necessary to recalculate the Young's Modulus, in order to calculate the deformations, as the part of the section under tensile stress will be in Zone 2 (light grey).

Leaving the whole section within 0.08 will not require a recalculation of the Young's Modulus, as the entire section will be in Zone 1 (white).

I-BEAM 152X76X10 → Massivity 200 m^{-1} → RF 30 min

d/λ=0.4 → d= 0.08m

d/λ=0.35 → d=0.07m

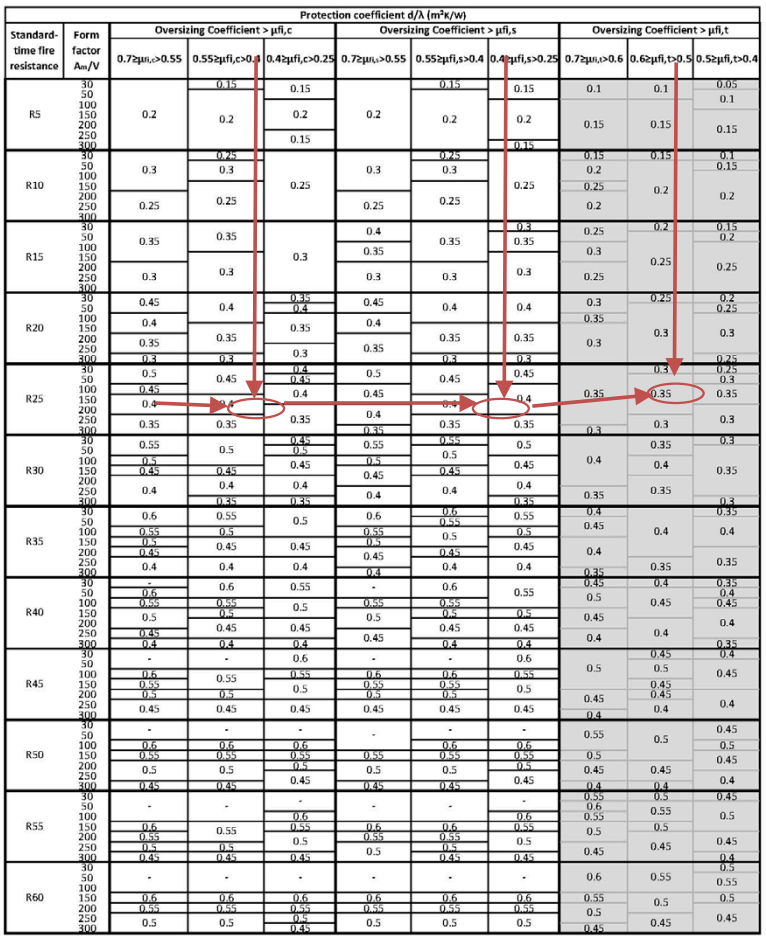

Protection coefficient d/λ (m^2K/W)											
Standard-time fire resistance	Form factor A_m/V	Oversizing Coefficient > μfi,c			Oversizing Coefficient > μfi,s			Oversizing Coefficient > μfi,t		
		0.7≥μfi,c>0.55	0.55≥μfi,c>0.4	0.4≥μfi,c>0.25	0.7≥μfi,s>0.55	0.55≥μfi,s>0.4	0.4≥μfi,s>0.25	0.7≥μfi,t>0.6	0.6≥μfi,t>0.5	0.5≥μfi,t>0.4
R5	30	0.2	0.15	0.15	0.2	0.15	0.15	0.1	0.1	0.05
	50									0.1
	100		0.2	0.2		0.2	0.2	0.15	0.15	
	150									0.15
	200			0.15			0.15			
	250									
	300									
R10	30	0.3	0.25	0.25	0.3	0.25	0.25	0.15	0.15	0.1
	50		0.3			0.3		0.2	0.2	0.15
	100							0.25		
	150		0.25			0.25		0.2		0.2
	200	0.25			0.25					
	250									
	300									
R15	30	0.35	0.35	0.3	0.4	0.35	0.3	0.25	0.2	0.15
	50				0.35		0.35	0.3	0.25	0.2
	100		0.3			0.3		0.25		0.25
	150	0.3			0.3		0.3			
	200									
	250									
	300									
R20	30	0.45	0.4	0.35	0.45	0.4	0.4	0.3	0.25	0.2
	50			0.4				0.35		0.25
	100	0.4		0.35	0.4				0.3	
	150		0.35			0.35	0.35	0.3		0.3
	200	0.35		0.3	0.35					
	250									
	300	0.3	0.3	0.4	0.3	0.3	0.3		0.3	0.25
R25	30	0.5	0.45	0.45	0.5	0.45	0.45			0.3
	50	0.45		0.4	0.45		0.4	0.35	0.35	0.35
	100	0.4	0.4			0.4				
	150			0.35	0.4				0.3	0.3
	200					0.35	0.35	0.3		
	250	0.35	0.35		0.35					
	300									
R30	30	0.55	0.5	0.45	0.55	0.55	0.5		0.35	0.3
	50	0.5		0.5		0.5		0.4	0.4	0.35
	100	0.45	0.45	0.45	0.5		0.45			
	150				0.45	0.45			0.35	
	200	0.4	0.4	0.4		0.4	0.4	0.35		
	250				0.4					
	300		0.35	0.35			0.35			0.3
R35	30	0.6	0.55	0.5	0.6	0.6	0.55	0.4	0.4	0.35
	50	0.55	0.5		0.55	0.55	0.5	0.45		0.4
	100	0.5		0.45	0.5	0.5			0.4	
	150	0.45	0.45				0.45	0.4		0.35
	200			0.4	0.45	0.45				
	250	0.4	0.4		0.4	0.4	0.4	0.35	0.35	
	300				0.4					
R40	30	-	0.6	0.55	-	0.6	0.55	0.45	0.4	0.35
	50	0.6						0.5	0.45	0.4
	100	0.55	0.55	0.5	0.55	0.55	0.5			0.45
	150	0.5	0.5		0.5	0.5		0.45	0.4	
	200		0.45	0.45		0.45	0.45			0.4
	250	0.45			0.45			0.4		
	300	0.4	0.4	0.4		0.4	0.4			0.35
R45	30	-	-	0.6	-	-	0.6	0.5	0.45	0.4
	50								0.5	0.45
	100	0.6	0.55	0.55	0.6	0.6	0.55			
	150	0.55		0.5	0.55	0.55	0.5		0.45	
	200	0.5	0.5		0.5	0.5		0.45	0.45	
	250	0.45	0.45	0.45	0.45	0.45	0.45		0.4	0.4
	300							0.4		
R50	30	-	-	-	-	-	-	0.55	0.5	0.45
	50				-					0.5
	100	0.6	0.6	0.6		0.6	0.6	0.5		
	150	0.55	0.55	0.55	0.55	0.55	0.55			0.45
	200	0.5	0.5	0.5	0.5	0.5	0.5	0.45	0.45	
	250			0.45			0.45			0.4
	300	0.45	0.45		0.45	0.45		0.4	0.4	
R55	30	-	-	-	-	-	-	0.55	0.5	0.45
	50							0.6	0.55	
	100			0.6			0.6	0.55		0.5
	150	0.6	0.55	0.55	0.6	0.6	0.55	0.5	0.5	
	200	0.55		0.5	0.55	0.55	0.5			0.45
	250	0.5	0.5		0.5	0.5		0.45	0.45	
	300	0.45	0.45	0.45		0.45	0.45			0.4
R60	30	-	-	-	-	-	-	0.6	0.55	0.5
	50									0.55
	100							0.55	0.5	0.5
	150	0.6	0.6	0.6	0.6	0.6	0.6			
	200	0.55	0.55	0.55	0.55	0.55	0.55	0.5	0.45	0.45
	250	0.5	0.5	0.5	0.5	0.5	0.5			
	300			0.45				0.45		

Figure 10. Application of the table for practical example

Some real cases of GFRP structures are presented in Figure 11.

5. Conclusions

- Having developed the fire design table and after searching for all tests performed to date, an important conclusion was that with the most common insulation thicknesses available for the type of application, GFRP + insulation sections cannot maintain their mechanical properties for exposure times longer than 60 minutes.
- If the temperature section remains between the glass transition, Tg, and the decomposition temperature, Td (Zone 2), the structure will probably be valid, but the modulus of elasticity of the section must be corrected (1).
- In contrast with the steel sections, the temperature within the GFRP section cannot be considered constant (due to its much lower thermal conductivity). A corrector equation (eq. 5) is proposed for GFRP sections exposed from the four sides, in order to obtain the maximum section temperature.
- After the calculation or dimensioning for a persistent situation and with the oversizing coefficients for the extraordinary fire situation, it is a straightforward task to obtain the necessary insulation thicknesses using the design table that has been proposed in this study.

6. References

References

2010. "Structural polymer components for building and construction. Draft, dimensioning and construction." .

Ascione, L, JF Caron, P Godonou, K Van IJselmuijden, J Knippers, T Mottram, M Oppe, M Gantriis Sorensen, J Taby, and L Tromp. 2016. "Prospect for new guidance in the design of FRP." *Support to the implementation, harmonization and future development of the Eurocodes. JRC Report EUR* 27666.

Associates, k. 2019. "http://www.tak2000.com/data/handbookx.pdf." USA.

Association, American Composites Manufactures, et al. 2012. "Pre-standard for load & resistance factor design (LRFD) of pultruded fiber reinforced polymer (FRP) structures." *Arlington, VA: ACMA* 14.

Bai, Yu, and Thomas Keller. 2007. "Modeling of post-fire stiffness of E-glass fiber-reinforced polyester composites." *Composites Part A: applied science and manufacturing* 38 (10): 2142–2153.

Bai, Yu, Thomas Keller, and Till Vallée. 2008. "Modeling of stiffness of FRP composites under elevated and high temperatures." *Composites Science and Technology* 68 (15-16): 3099–3106.

Bai, Yu, Nathan L Post, John J Lesko, and Thomas Keller. 2008. "Experimental investigations on temperature-dependent thermo-physical and mechanical properties of pultruded GFRP composites." *Thermochimica Acta* 469 (1-2): 28–35.

CEN, EN. 2005. "1-1-Eurocode 3: Design of steel structures-Part 1-1: General rules and rules for buildings." *European Committee for Standardization, Brussels* .

Correia, João R, Yu Bai, and Thomas Keller. 2015. "A review of the fire behaviour of pultruded GFRP structural profiles for civil engineering applications." *Composite Structures* 127: 267–287.

Correia, João R, Marco M Gomes, José M Pires, and Fernando A Branco. 2013. "Mechanical

Figure 11. Some real cases of GFRP structures

behaviour of pultruded glass fibre reinforced polymer composites at elevated temperature: Experiments and model assessment." *Composite Structures* 98: 303–313.

Council, National Research, et al. 2007. "Guide for the Design and Construction of Structures made of FRP Pultruded Elements." *CNR-DT* 205: 25–31.

Couto, Carlos, Élio Maia, Paulo Vila Real, and Nuno Lopes. 2018. "The effect of non-uniform bending on the lateral stability of steel beams with slender cross-section at elevated temperatures." *Engineering Structures* 163: 153–166.

Couto, Carlos, Paulo Vila Real, Nuno Lopes, and Bin Zhao. 2016. "Local buckling in laterally restrained steel beam-columns in case of fire." *Journal of Constructional Steel Research* 122: 543–556.

CUR Commission C124, The Netherlands, Gouda. 2003. "Fibre-Reinforced Polymers in Civil Load-Bearing Structures." .

del Hormigón Estructural, Instrucción. 2008. "EHE-08." *Madrid, Ministerio de Fomento, Secretaría General Técnica* .

Eurocode, EC. 1993. "3: Design of steel structures: Part 1.2, general rules–structural fire design." *Brussels: European Committee for Standardization. DD ENV* 1 (2).

Eurocode, EC. 2002. "1: Actions on structures: Part 1.2, General actions-Actions on structu res exposed to fi re." *Brussels: European Committee for Standardization* .

for Standardization (CEN), European Committee. 2004. "Eurocode 5—Design of timber structures, Part 1–2: General—Structural fire design." .

Franssen, Jean Marc, Venkatesh Kodur, and Raul Zaharia. 2009. *Designing steel structures for fire safety*. CRc Press.

Franssen, Jean-Marc, Bin Zhao, and Thomas Gernay. 2016. "Experimental tests and numerical modelling on slender steel columns at high temperatures." *Journal of Structural Fire Engineering* 7 (1): 30–40.

Garmendia, Iñaki, Eva Anglada, Haritz Vallejo, and Miguel Seco. 2016. "Accurate calculation of conductive conductances in complex geometries for spacecrafts thermal models." *Advances in Space Research* 57 (4): 1087–1097.

Jandera, Michal, Martin Prachař, and František Wald. 2020. "Lateral-torsional buckling of class 4 section uniform and web tapered beams at elevated temperature." *Thin-Walled Structures* 146: 106458.

Keller, Thomas, Craig Tracy, and Aixi Zhou. 2006. "Structural response of liquid-cooled GFRP slabs subjected to fire–Part II: Thermo-chemical and thermo-mechanical modeling." *Composites Part A: applied science and manufacturing* 37 (9): 1296–1308.

Knobloch, Markus, Diego Somaini, Jacqueline Pauli, and Mario Fontana. 2012. "Numerical analysis and comparative study of the cross-sectional capacity of structural steel members in fire." *Journal of Structural Fire Engineering* 3 (1): 19–36.

Maia, Élio, Carlos Couto, Paulo Vila Real, and Nuno Lopes. 2016. "Critical temperatures of class 4 cross-sections." *Journal of Constructional Steel Research* 121: 370–382.

Maraveas, Chrysanthos, Konstantinos Miamis, and Apostolos A Vrakas. 2012. "Fiber-reinforced polymer-strengthened/reinforced concrete structures exposed to fire: a review." *Structural engineering international* 22 (4): 500–513.

Morgado, T, JR Correia, N Silvestre, and FA Branco. 2018. "Experimental study on the fire resistance of GFRP pultruded tubular beams." *Composites Part B: Engineering* 139: 106–116.

Morgado, T, N Silvestre, and JR Correia. 2018a. "Simulation of fire resistance behaviour of pultruded GFRP beams–Part I: Models description and kinematic issues." *Composite Structures* 187: 269–280.

Morgado, T, N Silvestre, and JR Correia. 2018b. "Simulation of fire resistance behaviour of pultruded GFRP beams–Part II: Stress analysis and failure criteria." *Composite Structures* 188: 519–530.

Prachar, Martin, Michal Jandera, Frantisek Wald, and Bin Zhao. 2015. "Lateral Torsional-Buckling of Class 4 Steel Plate Beams at Elevated Temperature: Experimental and Numerical Comparison." *Journal of Structural Fire Engineering* 6 (3): 223–236.

Rosa, IC, JP Firmo, JR Correia, and JAO Barros. 2019. "Bond behaviour of sand coated GFRP bars to concrete at elevated temperature–Definition of bond vs. slip relations." *Composites Part B: Engineering* 160: 329–340.

Rosa, IC, T Morgado, JR Correia, JP Firmo, and N Silvestre. 2018. "Shear Behavior of GFRP Composite Materials at Elevated Temperature." *Journal of Composites for Construction* 22 (3): 04018010.

Standard, International. 1999. "Fire-resistance tests elements of building construction. Part 1: General requirements." .

Wang, Ke, Ben Young, and Scott T Smith. 2011. "Mechanical properties of pultruded carbon fibre-reinforced polymer (CFRP) plates at elevated temperatures." *Engineering Structures* 33 (7): 2154–2161.

Wickström, Ulf. 1985. "Temperature analysis of heavily-insulated steel structures exposed to fire." *Fire Safety Journal* 9 (3): 281–285.

Wong, PMH, JM Davies, and YC Wang. 2004. "An experimental and numerical study of the behaviour of glass fibre reinforced plastics (GRP) short columns at elevated temperatures." *Composite structures* 63 (1): 33–43.

Yu, Bai, Vallee Till, and Keller Thomas. 2007. "Modeling of thermo-physical properties for FRP composites under elevated and high temperature." *Composites Science and Technology* 67 (15-16): 3098–3109.